Available online at www.sciencedirect.com
ScienceDirect
Journal of Power Sources 162 (2006) 160–164
JOURNAL OF POWER SOURCES
www.elsevier.com/locate/jpowsour

Short communication

A novel catalyst support for DMFC: Onion-like fullerenes

Bingshe Xu [a,b,*], Xiaowei Yang [a], Xiaomin Wang [a,b], Junjie Guo [a], Xuguang Liu [b]

[a] College of Materials Science and Engineering, Taiyuan University of Technology, Taiyuan 030024, China
[b] Key Laboratory of Interface Science and Engineering in Advanced Materials, Taiyuan University of Technology, Ministry of Education, Taiyuan 030024, China

Received 22 April 2006; received in revised form 21 June 2006; accepted 21 June 2006
Available online 9 August 2006

Abstract

Onion-like fullerenes (OLFs) were employed as the support for Pt in direct methanol fuel cells (DMFCs). A Pt/OLFs catalyst was synthesized by an impregnation–reduction method. Its structure and morphology were characterized by XRD, HRTEM and XPS. The Pt nanoparticles uniformly dispersed on OLFs had an average diameter of 3.05 nm, compared to 4.10 nm in Pt/Vulcan XC-72 prepared by the same method. XPS analysis revealed that Pt/OLF contained mostly Pt(0), with traces of Pt(II) and Pt(IV). Cyclic voltammetry showed that the real surface area of the Pt/OLFs was larger than Pt/XC-72 and the electrocatalytic activity of the Pt/OLFs catalyst, from the peak current value at around 0.78 V, outperformed the Pt/Vulcan XC-72 by about 20% in the electrooxidation of methanol.

Keywords: Pt/onion-like fullerenes (Pt/OLFs); Characterization; Electrocatalytic activity

1. Introduction

In recent years, direct methanol fuel cells (DMFC) have been considered as one of the most promising power sources. In order to improve the performance of a DMFC, improvements in the catalyst layer have to be considered [1]. Among these, good properties of the catalyst supports, such as stability in both acidic and basic media, high specific surface area and a good electric conductivity are essential for the Pt catalyst to produce high catalytic activity [2,3]. It has been proven that the structure of the carbon supports, such as carbon black [4], CNTs [5], or graphite nanofibres [6] influence the structure of the catalyst layer and, as a result, the electrochemical performance of the catalyst. However, there are few reports of onion-like fullerenes as a catalyst support.

Since Ugarte's discovery in 1992 [7], onion-like fullerenes (OLFs) have been a subject of great interest given their unique structure and physical properties [8,9]. Many potential applications, such as nano ball-bearings, nano-electronic-magnetic devices, gas storage and biotechnology [10–12] have been proposed. They can be employed as a good support for catalysts, where the active metal particles disperse on the external shells, and provide goos corrosion-resistance, high conductivity and a relatively large specific surface area [13].

In the present study, a Pt/OLFs catalyst was prepared by the method of impregnation–reduction. The morphology was characterized by many methods and its catalytic activity for the electrooxidation of methanol was obtained.

2. Experimental

2.1. Preparation of the Pt/OLFs catalyst

The OLFs with a diameter of about 30 nm were prepared by chemical vapor deposition (CVD) and the synthesis OLFs was similar to that reported in a previous paper [14].

The pretreatment and metal deposition procedure on OLFs was similar to that reported by Dam et al. [15]. The OLFs were first refluxed in the nitric acid (5 mol L^{-1}) at 120 °C for 8 h. Functional groups were introduced on the surface of OLFs during this step. Metal was introduced to the surface-oxidized OLFs by reduction of H_2PtCl_6 in formaldehyde for 8 h. The wet solids were washed several times with deionized water, filtered and dried overnight at 80 °C in a vacuum oven. A final Pt/OLFs with a metal loading of 20 wt.% was obtained. A Pt/Vulcan XC-72 catalyst was also prepared by the same method.

* Corresponding author. Tel.: +86 351 6010311; fax: +86 351 6010311.
E-mail address: xubs@public.ty.sx.cn (B. Xu).

0378-7753/$ – see front matter © 2006 Elsevier B.V. All rights reserved.
doi:10.1016/j.jpowsour.2006.06.063

2.2. Characterization of the Pt/C

The samples were examined by high resolution transmission electron microscopy (HRTEM) on a JEOL JEM-2010 and with a scanning electron microscope, JEOL JSM-6700, to characterize the morphology and to determine the composition of the elements in the catalysts. More than 300 particles were used to obtain information on the distribution and size of the Pt. X-ray diffraction (XRD) measurements were carried out with Cu Kα radiation to characterize the structure of the catalyst.

X-ray photoelectron spectroscopy data were obtained with an ESCALab220i-XL electron spectrometer from VG Scientific using 300 W Al Kα radiation. The base pressure was about 3×10^{-9} mbar. Spectra were recorded at the C 1s and Pt 4f photoelectron peaks. The internal standard peak for determining the binding energies was that of carbon C 1s (284.6 eV).

2.3. Preparation and characterization of the electrode

An electrochemical instrument (Autolab PGSTAT302) and a conventional three-electrode test cell with saturated calomel electrode (SCE) as the reference electrode and platinum foil as the counter electrode were used for the electrochemical measurements. The working electrode was a thin layer of Nafion-impregnated catalyst cast onto a vitreous carbon disc with a diameter of 4 mm. The catalyst layer resembled that in a previous paper [16]. The Pt/C loading on the electrodes was approximately 1.5 mg cm^{-2}. A solution of 1.0 M H_2SO_4 or 2.0 M CH_3OH/1.0 M H_2SO_4 was used as the electrolyte. All the reagents used were of analytical grade. The electrolytes were degassed with nitrogen for 30 min prior to electrochemical measurements.

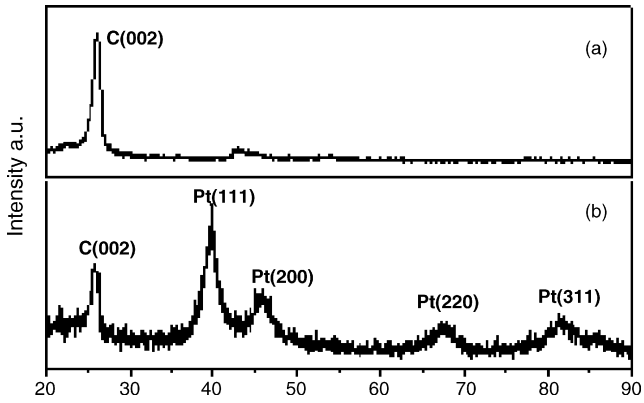

Fig. 1. XRD patterns of OLFs (a) and Pt/OLFs (b).

3. Results and discussions

3.1. Characterizations of Pt/C catalysts

The XRD pattern of the raw OLFs and Pt/OLFs are shown in Fig. 1. The intrinsic peak of the raw OLFs is observed at ca. 26 °C and Pt/OLFs also have that peak in the same position, indicating that the use of nitric acid for the pre-treatment of OLFs does not

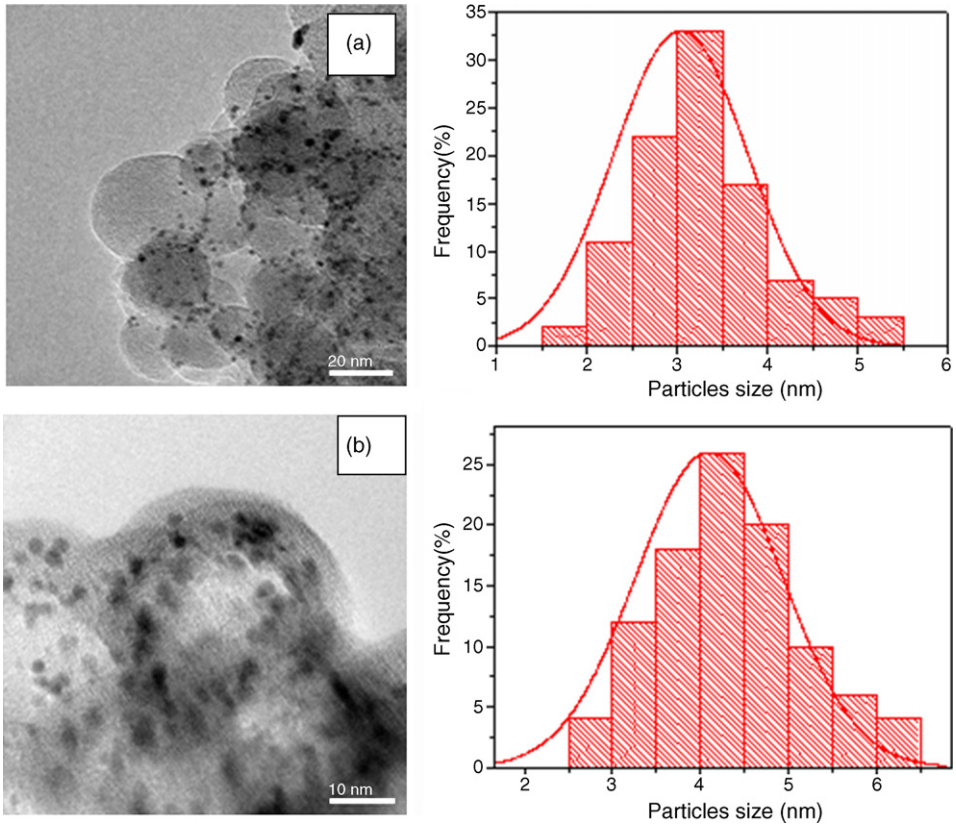

Fig. 2. HRTEM images of Pt/OLFs (a) and Pt/Vulcan XC-72 (b) and their corresponding size distribution histograms.

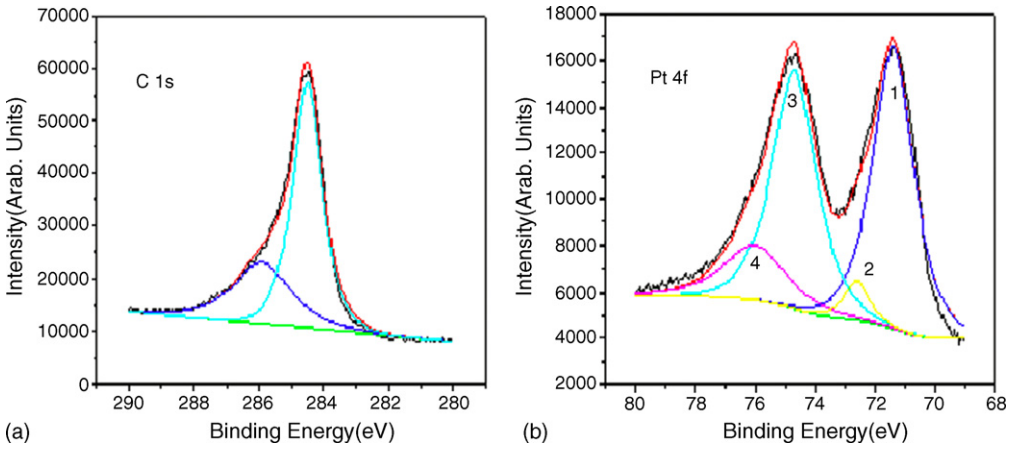

Fig. 3. The C 1s (a) and Pt 4f (b) regions of the XPS spectrum of the Pt/OLFs.

affect the position of this peak. It is inferred that reflux with nitric acid makes no change in the crystallinity of OLFs. Moreover, Pt/OLFs display the characteristic patterns of Pt fcc diffraction. The 2θ values are: Pt(1 1 1) = 39.95°, Pt(2 0 0) = 45.80°, Pt(2 2 0) = 67.95° and Pt(3 1 1) = 81.45°. The broader diffraction peaks for the particles also lead to a smaller average particle size as calculated from the Scherrer equation [17]:

$$L = \frac{0.9\lambda_{K\alpha 1}}{(B_{2\theta}\cos\theta_B)} \quad (1)$$

where L is the average particle size, $\lambda_{K\alpha 1}$ the X-ray wavelength (1.54056 Å for Cu Kα1 radiation), $B_{2\theta}$ the peak broadening and θ_B is the angle corresponding to the peak maximum. The average size is calculated to be 3.0 ± 0.3 nm for Pt/OLFs.

Fig. 2a shows a HRTEM image of the 20 wt.% Pt/OLFs. The spherical platinum particles on OLFs are uniform with good distribution. Based on the measurements of 300 particles in random regions, the average particle size is estimated to be 3.05 nm, in good agreement with the results from XRD. The corresponding histogram reveals that the particle size distribution is rather narrow and exhibits the features of a log-normal distribution. The particle size of Pt may be correlated with the oxidation of OLFs, which indicates that the efficient deposition of Pt nanoparticles is due to a strong interaction between the metal salt precursor and the shells of the OLFs. Chemical functional groups, namely –COOH and –OH derived from the HNO_3 refluxing process, act as anchoring sites for the Pt nanoparticles, inducing the formation of small particles [18]. Stonehart [19] found that particle sizes between 3 and 5 nm yield a good oxygen reduction activity, with decreasing activity for both smaller and lager sizes. Hence, the size distribution found here is in an ideal range to get good performance for the catalyst in DMFC electrodes. The average particle size of Pt is estimated to be 4.10 nm for Pt/Vulcan XC-72, 1.05 nm larger than that for Pt/OLFs.

XPS is used to determine the surface oxidation states of the metals. As most of the atoms in small particle clusters are surface atoms, the oxidation state measured as such would also reflect the bulk oxidation state. The XPS spectrum of Pt/OLFs is given in Fig. 3. The C 1s spectrum, deconvolutes into two peaks and is presented in Fig. 3a. The peak at 284.8 eV shows that the surfaces are covered with carboxylic groups. The C 1s spectrum appears to be composed of graphitic carbon (284.5 eV) and –C=O like species (286.1 eV) [20].

The Pt 4f core level XPS spectrum of Pt/OLFs is shown in Fig. 3b. The doublet contains a peaks at 71.4 and 74.7 eV, i.e., there is spin–orbit splitting of 3.3 eV for the different Pt oxidation states of the Pt(0) and Pt(IV) species. The lower binding energy doublet with Pt $4f_{7/2}$ at 71.4 eV agrees well with the published value of 71.1 eV for Pt. The slight shift in the Pt(0) peak to a higher binding energy is a known effect for small particles, as reported by Roth et al. [21]. The spectrum is deconvoluted using a curve-fitting program into four components labeled as 1, 2, 3 and 4 with respective binding energies of 71.3, 72.6, 74.7 and 76.0 eV. The signals at 71.3 eV can be assigned to zero-valent Pt, the signal at 72.6 eV is ascribed to PtO and $Pt(OH)_2$, and the signals at 74.7 and 76.0 eV seemingly arise from PtO_2 species [20,21]. The shift to a higher binding energy in the Pt/OLFs may be due to electronic effects produced by the presence of very small and highly dispersed Pt particles on the OLFs. This is because neighbor atoms are fewer in the dispersed system than in the bulk, so that electrons are also fewer. This results in a less effective screening, and the BE of the orbital shifts to a higher energy [22].

3.2. Electrochemical properties of Pt/C catalysts

Well-defined hydrogen absorption–desorption features are seen in the cyclic voltammogram curve of the Pt/OLFs electrode in 1.0 M H_2SO_4 solution at room temperature (Fig. 4). The real surface area of platinum for the Pt/OLFs catalysts could be estimated from the integrated charge in the hydrogen absorption region of the cyclic voltammogram. This area is normalized to the mass of Pt in the catalyst (S_S specific surface area). S_S is be obtained from

$$S_S = \frac{Q_H}{M_{Pt}Q_{Href}} \quad (2)$$

where Q_H is the amount of charge of the electroabsorption of hydrogen atoms on the Pt surface, M_{Pt} the mass of Pt and Q_{Href} is assumed to be 0.21 mC cm^{-2} corresponding to a surface density

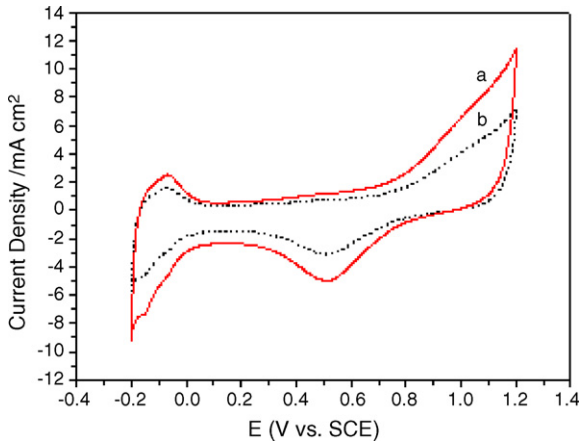

Fig. 4. Cyclic voltammogram curves of the Pt/OLFs electrodes in 1.0 M H_2SO_4 solution at room temprature at scan rate of 50 mV s^{-1}: (a) Pt/OLFs and (b) Pt/Vulcan XC-72.

Table 1
The real (active) surface areas of Pt/Vulcan XC-72 and Pt/OLFs catalysts as determined by hydrogen electroabsorption

Catalyst	Content of Pt (wt.%)	Pt loading (μg per 0.126 cm^2)	Q_H (mC)	S_s (m^2 g^{-1})
Pt/OLFs	18.8	35.5	3.2	42.9
Pt/Vulcan XC-72	18.2	34.4	2.4	33.2

of 1.3×10^{15} atom cm^{-2} of Pt [23]. The values of S_S of the as-prepared catalysts are listed in Table 1. It is not surprising that there is a difference in the real surface areas because the average sizes of the Pt particles in two catalysts are different.

Fig. 5 shows the cyclic voltammograms of Pt/OLFs and Pt/Vulcan XC-72 paste electrodes in 2 M CH_3OH + 1 M H_2SO_4 aqueous solutions, respectively. From curve a in Fig. 5, two peaks for methanol oxidation of Pt/OLFs can be observed. The anodic peak at around 0.57 V in the reverse scan may be associated with the reactivation of oxidized Pt. The current peak at about 0.78 V in the forward scan is attributed to methanol electrooxidation on the Pt catalyst [24]. Fig. 5 clearly shows that this peak is significantly higher in the Pt/OLFs catalyst than that in the Pt/Vulcan XC-72 catalyst. The specific activity of the Pt/OLFs catalyst, which is evaluated by the peak current value at around 0.78 V, outperformed the Pt/Vulcan XC-72 by ca. 20%. It is well known that the catalytic activity of metal particles depends strongly on the particle size and distribution. The smaller the catalyst particles, the higher is usually their catalytic activity [25]. The Pt/OLFs catalyst exhibits a higher catalytic activity than Pt/Vulcan XC-72 in the electrooxidation of methanol because of its smaller particle size.

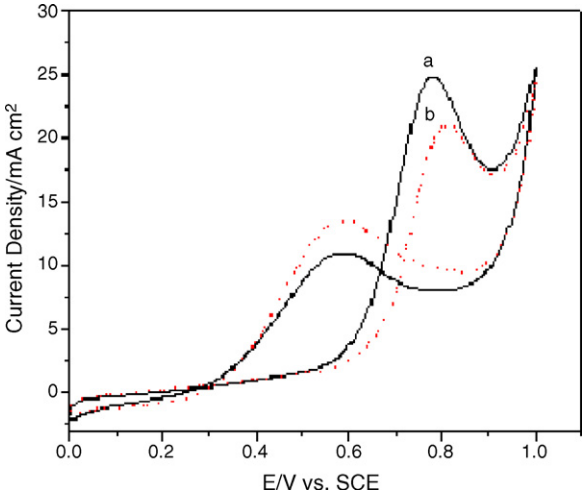

Fig. 5. Cyclic voltammograms of the different electrodes in 1.0 M H_2SO_4 + 2.0 M CH_3OH solution at room temprature at scan rate of 50 mV s^{-1}: (a) Pt/OLFs and (b) Pt/Vulcan XC-72.

4. Conclusions and summary

A 20 wt.% Pt/OLFs and Pt/Vulcan XC-72 catalysts were synthesized by an impregnation–reduction method. The Pt/OLFs shows the characteristic diffraction peaks of a Pt fcc structure. The Pt nanoparticles are highly dispersed on OLFs and have an average diameter of 3.05 nm, compared to 4.10 nm on Vulcan XC-72. XPS analysis reveals that the catalyst contained mostly Pt(0), with traces of Pt(II) and Pt(IV). The real surface area of Pt on the Pt/OLFs is larger than Pt/XC-72 due to its smaller average particle size. The catalytic activity of the Pt/OLFs catalysts for methanol electro-oxidation, as measured by cyclic voltammetrys is evaluated from the peak current value at around 0.78 V, and outperformed the Pt/Vulcan XC-72 by about 20%. The results show that the Pt/OLFs might be a good candidate for a catalyst in DMFC applications.

Acknowledgements

The authors acknowledge financial support from National Basic Research Program of China (Grant no. 2004CB217808), Key Project of National Natural Science Foundation of China (Grant no. 90306014), National Natural Science Foundation of China (Grant no. 20471041), Natural Science Foundation of Shanxi Province (2006011054) and Science Foundation of Shanxi Educational Office (20051214).

References

[1] A. Gamez, D. Richard, P. Gallezot, et al., Electrochim. Acta 41 (1996) 307.
[2] J.S. Yu, S. Kang, S.B. Yoon, G. Chai, J. Am. Chem. Soc. 124 (2002) 9382.
[3] H.S. Liu, C.J. Song, L. Zhang, et al., J. Power Sources 155 (2006) 95.
[4] F. Cloaguen, J. Leger, C. Lamy, J. Appl. Electrochem. 27 (1997) 1052.
[5] S.H. Joo, S.J. Choi, H. Oh, et al., Nature 412 (2001) 169.
[6] C.A. Bessel, K. Laubernds, N.M. Rodriguez, et al., J. Phys. Chem. B 105 (2001) 1115.
[7] D. Ugarte, Nature 359 (1992) 707.
[8] R. Ruoff, D.C. Lorents, B. Chan, et al., Science 259 (1993) 346.
[9] B.S. Xu, J.J. Guo, X.M. Wang, et al., Carbon 44 (2006) 2631–2634.
[10] L. Rapport, Y. Bilik, Y. Feldman, et al., Nature 12 (1997) 3328.
[11] R.K. Rana, Y. Koltypin, A. Gedanken, Chem. Phys. Lett. 344 (2001) 256.
[12] B.S. Xu, Y.T. Fan, G.H. Liu, et al., Carbon 44 (2006) 1845.
[13] N. Sano, H. Wang, I. Alexandrou, et al., J. Appl. Phys. 92 (2002) 2783.
[14] X.M. Wang, B.S. Xu, X.G. Liu, et al., Diam. Relat. Mater. 15 (2006) 147.
[15] H.E. Dam, H.V. Bekkum, J. Catal. 131 (1991) 335.

[16] R.Z. Yang, X.P. Qiu, H.R. Zhang, et al., Carbon 43 (2005) 11–16.
[17] B.E. Warren, X-ray Diffraction, Addison-Wesley, Reading, MA, 1996.
[18] N. Rajalakshmi, H. Ryu, M.M. Shaijumon, et al., J. Power Sources 140 (2005) 250.
[19] P. Stonehart, J. Appl. Electrochem. 22 (1992) 995.
[20] A.K. Shukla, M.K. Ravikumar, A. Roy, et al., J. Electrochem. Soc. 141 (1994) 1517.
[21] C. Roth, M. Goetz, H. Fuess, J. Appl. Electrochem. 31 (2001) 793.
[22] Z. Koĭnya, J. Kiss, A. Oszkoĭ, et al., Phys. Chem. Chem. Phys. 3 (2001) 155.
[23] G. Faubert, D. Guay, J.P. Dodelet, J. Electrochem. Soc. 145 (1998) 2985.
[24] F.B. Su, J.H. Zeng, Y.S. Yu, et al., Carbon 43 (2005) 2366.
[25] X. Li, W.X. Chen, J.Z., et al., Carbon 43 (2005) 2168.